Breast Tumor Microenvironment in Black Women: A Distinct Signature of CD8+ T Cell Exhaustion

Supplementary Methods

Patient population

The data and tumor specimens for this study were drawn from the Women's Circle of Health (WCHS), which was a multi-site case-control study designed specifically to examine risk factors for aggressive breast cancer in Black and White women. Eligible women were 20-75 years old, self-identified as Black or White, and had primary, histologically confirmed breast cancer, and no previous history of cancer other than non-melanoma skin cancer. Cases were first identified from hospitals in metropolitan New York City; since 2006, the New Jersey State Cancer Registry (NJSCR) identified eligible patients using rapid case ascertainment. Upon consent, an in-depth at-home interview was conducted to collect data on established and suspected risk factors for breast cancer, and cases signed a release for their formalin-fixed paraffin-embedded (FFPE) tumor blocks and medical records. From 2008, enrollment was limited to only Black women in New Jersey and since 2013, the study has been enrolling newly diagnosed Black women with breast cancer through NJSCR into a follow-up study (WCHSFS). Methods have been described in detail for WCHS [1] and WCHSFS [2]. With the expansion to focus on survivorship in the WCHFS, detailed information was collected on obesity-related comorbidities and their management, health related quality of life, lifestyle and social determinants of health, medication adherence, and new breast cancer events, as well as pharmacy records.

Clinicopathological variables, including tumor grade, tumor size, lymph node status, stage, and status of estrogen receptor (ER), progesterone receptor (PR), and human epidermal growth factor receptor 2 (HER2) were obtained from pathology reports. Molecular subtypes were defined as hormone receptor-positive (HR+, i.e., ER+ and/or PR+)/HER2+, HR+/HER2-, HR-/HER2+, and HR-/HER2-, i.e., triple-negative tumors.

Vital status and causes and date of death are ascertained through linkage with NJSCR files, which are updated annually using various sources including state and the National Death Index, hospital discharge files, Medicare and Medicaid files, and Social Security Administrative Data. Hospitals also submit annual vital status updates, and NJSCR uses information from e-path to update vital status.

Pathological assessment of tumor infiltrating lymphocytes (TILs)

As part of the protocol of receiving unstained slides and tumor blocks for tumor microarray construction in the WCHS, hematoxylin and eosin (H&E) stained sections were prepared. These sections were used for histopathologic scoring of TIL-str by a board-certified breast pathologist (T.K.). TIL-str was scored for the stromal area occupied by mononuclear inflammatory cells over total intratumoral area between 0% and 100%, and rounded up to the nearest 10%, as recommended by the International TILs Working Group [3]. The rater was blinded to patients' age, race, and clinicopathological characteristics. In our experience, the agreement for TIL-str

scores between two raters was substantial (weighted kappa = 0.66 and 0.71 for two sections from 100 cases) [4]. For the current analysis, *in situ* cases were excluded and a total of 1,315 invasive cases with TILs evaluated were included, consisting of 920 Black and 395 White women with breast cancer. Descriptive characteristics of the patients included in pathological TIL analysis are summarized in **Table 1**.

Immunohistochemical (IHC) staining of $CD4^+$ T cells

Tumor tissue microarrays (TMAs) were built for WCHS cases using FFPE tumor blocks. H&E sections were reviewed by study pathologist (T.K.) and high tumor content areas were circled for TMA cores to be taken. The cores ranged in size from 0.6 mm to 1.2 mm in diameter and most patient tumors were represented by at least two TMA cores. IHC assays for CD4 were performed by the Pathology Network Shared Resource (PNSR) at Roswell Park Comprehensive Cancer Center. TMA sections were cut at 4 μm, placed on charged slides, and dried at 60°C for one hour. Slides were cooled to room temperature, placed on the Dako Omnis autostainer, and stained with the accompanying Dako antibody and secondary reagents following manufacturer recommendations. TRS High was used for epitope retrieval for 30 minutes and the CD4 antibody was applied. DAB (Diaminobenzidine) was applied for marker visualization. Stained TMA slides were digitally scanned using Aperio Scanscope with 20x bright-field microscopy and then viewed using Spectrum, a web-based digital pathology system. Aperio ImageScope was used to view images, create annotation layers, and circle areas of interest for analysis. The Aperio platform was used to develop quantitative image analysis algorithm macros to score IHC slides, which output the total number of analyzed cells, the percentage of $CD4^+$ cells, and the size of the tissue area that was analyzed. In order to normalize the variable results produced due to the difference in tissue core sizes, the number of $CD4^+$ T cells in each core was reported per square millimeter of tumor tissue. Cores lacking sufficient tumor cellularity (<20 tumor nuclei per core) were excluded from the analysis. A total of 659 patients (n=551 Black, 108 White women) were included in the final analysis of $CD4^+$ T cells by IHC staining.

NanoString PanCancer Immune Panel gene expression assays

NanosString PanCancer Immune Panel is a nCounter® technology-based, multiplexed gene expression panel designed to quantitate 770 genes to identify various immune cell subsets and assess immunological functions. Two x 10-micron whole section curls cut from tumor blocks from each case were used for RNA extraction using Roche High Pure FFPET RNA Isolation Kit. RNA samples were quantitated using Qubit method and fragmentation analysis was performed using Agilent TapeStation. To improve the power for comparisons between Black and White breast cancer patients and minimize potential confounding effects by tumor subtypes, tumors from patients with HER2+ and triple negative breast cancer were over sampled from WCHS and supplemented with eligible cases from Roswell Park PNSR. Black and White cases were also frequency matched on age at diagnosis, tumor grade, and IHC subtypes defined by ER, PR, and HER2 status. A total of 190 Black and 177 White breast cancer cases, plus 15 technical duplicates and one biological trio (from three different tumor blocks of a same case), were submitted for the nCounter assay performed by Roswell Park Genomic Shared Resource (GSR).

All samples passed the QC measures following manufacturer's recommendations. Between each of the technical duplicative pairs, the correlations of the gene counts were in the range of 0.98-0.99, with one exception of an R=0.89. The correlations of the gene counts among the biological trio samples were in the range of 0.98-0.99. Data were first normalized to positive controls included in the assays, and then a panel of 40 house-keeping genes using geNorm algorithm [5], and also log2-transformed before further analysis.

Deconvolution analysis of immune cells in tumor microenvironment based on gene expression data

Several deconvolution algorithms based on gene expression data have been published to infer cell composition from bulk tissue gene expression data. Since NanoString PanCancer Immune Panel was developed based on a statistical method described in the paper by Danaher et al [6] and validated using tumor transcriptomic data from TCGA, we followed the same principles in our deconvolution analysis. A salient feature of this method is the requirement of a co-expression pattern with strong correlations among all markers selected for each immune cell subset with a regression coefficient (slope) of one. We used nSolver with Advanced Analysis module from NanoString to select cell type markers that fit the required criteria. We further applied two commonly used deconvolution algorithms, CIBERSORT [7] and xCell [8], to our data and estimated the proportions of various immune cell subsets permitted by the programs. A final set of 10 immune cell subsets and their markers were chosen, which reached a minimum correlation of 0.6 between Danaher algorithm and at least one of CIBERSORT or xCell algorithm. These 10 immune cell subsets (selected cell-specific marker genes) are: total T cells (*CD6, CD3D, CD3E, SH2D1A, TRAT1, CD3G*), $CD8^+$ T cells (*CD8A, CD8B*), CD4+ T cells (total T cell score minus $CD8^+$ T cell score), regulatory T cells (*FOXP3*), B cells (*BLK, CD19, FCRL2, MS4A1, KIAA0125, TNFRSF17, TCL1A, SPIB, PNOC*), macrophages (*CD68, CD84, CD163, MS4A4A*), neutrophils (*FPR1, SIGLEC5, CSF3R, FCAR, FCGR3B, CEACAM3, S100A12*), mast cells (*TPSB2, TPSAB1, CPA3, MS4A2, HDC*), dendritic cells (*CCL13, CD209, HSD11B1*), and natural killer (NK) cells (*XCL1, XCL2, NCR1*).

The *absolute fractions*, which were calculated as the average levels of the selected cell type-specific marker genes, provide an estimate of the fraction of an immune cell type relative to all cells, including tumor and normal epithelial cells, immune cells, and other stromal cells, present in the bulk tissue. We also derived the *relative fractions*, which were calculated as the ratios between a cell type score and the total tumor infiltrating leukocytes estimated by $CD3^+$ expression. The *relative fractions* provide an estimate of the fraction of an immune cell type relative to all types of infiltrating immune cells in tumor microenvironment. We then analyzed the absolute fractions and the relative fractions of the immune cells in relation to tumor ER, PR, and HER2 status. Because the absolute fractions were heavily affected by those tumor features whereas the relative fractions remained unaffected, we chose to use the relative fractions for the bulk of the analyses, unless otherwise specified.

Estimation of B cell receptor (BCR) and T cell receptor (TCR) repertoire in TCGA

BCR and TCR diversity scores (richness, evenness, and Shannon entropy) of breast tumors in TCGA were obtained from the resource paper by Thorsson et al [9]. Briefly, TCR CDR3

sequences were identified from bulk tumor RNA-seq data using MiTCR v1.0.3 [10] and parameters to optimize the extraction from RNA-seq datasets previously described by Brown et al. [11]. BCR inference from tumor RNA-seq data was performed using the V'DJer tool [12] to reconstruct the immunoglobulin heavy chain. RSEM v1.2.21 [13] was used to quantify the BCR contigs; IMGT/HighV-Quest [14] was used to identify V and J gene segments, CDR3 sequence and V region identity for each contig.

Statistical analysis

Comparisons of tumor immune phenotypes between Black and White patients were conducted using Wilcoxon tests which controlled for hormone receptor (HR) status (estrogen receptor and progesterone receptor) in multivariable linear regression models. Considering the varying scales of different immune cell subsets, we centered the data to have an overall mean of 0 for each cell subset before calculating the subgroup medians by race (White vs. Black) and the differences in subgroup medians were then plotted, along with p-values derived from Wilcoxon tests. Multiple testing errors were controlled for using Bonferroni correction based on the number of cell subsets analyzed (0.05/11).

To visualize differences in immune cell scores between Black and White patients after controlling for hormone receptor (HR) status, standardized residuals for each racial group were derived from multivariable linear regression models containing the immune cell scores as dependent variables and race and tumor HR status as independent variables.

For survival analysis, follow up began at the time of breast cancer diagnosis and ended at the time of last contact or the occurrence of death. Patients still alive were censored at the time of last contact. The mean follow-up time (range) of TCGA, WCHS and METABRIC was 27 (0-287) months, 72 (9-153) months, and 115 (0-355) months, respectively. For all-cause mortality, Cox proportional hazard models were used to derive hazard ratios (HRs) and 95% confidence intervals (CIs) with controlling for covariates. For breast cancer-specific mortality, deaths due to non-breast cancer-related causes were analyzed as competing risk in the models using `cmprsk` R package and subdistribution HRs (SHRs) and corresponding 95% CIs were derived. The proportional hazards assumption was examined by the scaled Schoenfeld residuals, and no violation was identified in any of the models.

References cited in Supplementary Methods:

1. Ambrosone CB, Ciupak GL, Bandera EV*, et al.* Conducting Molecular Epidemiological Research in the Age of HIPAA: A Multi-Institutional Case-Control Study of Breast Cancer in African-American and European-American Women. J Oncol 2009;2009:871250.
2. Bandera EV, Demissie K, Qin B*, et al.* The Women's Circle of Health Follow-Up Study: a population-based longitudinal study of Black breast cancer survivors in New Jersey. J Cancer Surviv 2020;14(3):331-346.
3. Salgado R, Denkert C, Demaria S*, et al.* The evaluation of tumor-infiltrating lymphocytes (TILs) in breast cancer: recommendations by an International TILs Working Group 2014. Ann Oncol 2015;26(2):259-71.

4. Khoury T, Peng X, Yan L*, et al.* Tumor-Infiltrating Lymphocytes in Breast Cancer: Evaluating Interobserver Variability, Heterogeneity, and Fidelity of Scoring Core Biopsies. Am J Clin Pathol 2018;150(5):441-450.
5. Vandesompele J, De Preter K, Pattyn F*, et al.* Accurate normalization of real-time quantitative RT-PCR data by geometric averaging of multiple internal control genes. Genome Biol 2002;3(7):RESEARCH0034.
6. Danaher P, Warren S, Dennis L*, et al.* Gene expression markers of Tumor Infiltrating Leukocytes. J Immunother Cancer 2017;5:18.
7. Newman AM, Liu CL, Green MR*, et al.* Robust enumeration of cell subsets from tissue expression profiles. Nat Methods 2015;12(5):453-7.
8. Aran D, Hu Z, Butte AJ. xCell: digitally portraying the tissue cellular heterogeneity landscape. Genome Biol 2017;18(1):220.
9. Thorsson V, Gibbs DL, Brown SD*, et al.* The Immune Landscape of Cancer. Immunity 2018;48(4):812-830 e14.
10. Bolotin DA, Shugay M, Mamedov IZ*, et al.* MiTCR: software for T-cell receptor sequencing data analysis. Nat Methods 2013;10(9):813-4.
11. Brown SD, Raeburn LA, Holt RA. Profiling tissue-resident T cell repertoires by RNA sequencing. Genome Med 2015;7:125.
12. Mose LE, Selitsky SR, Bixby LM*, et al.* Assembly-based inference of B-cell receptor repertoires from short read RNA sequencing data with V'DJer. Bioinformatics 2016;32(24):3729-3734.
13. Li B, Dewey CN. RSEM: accurate transcript quantification from RNA-Seq data with or without a reference genome. BMC Bioinformatics 2011;12:323.
14. Lefranc MP, Giudicelli V, Ginestoux C*, et al.* IMGT, the international ImMunoGeneTics information system. Nucleic Acids Res 2009;37(Database issue):D1006-12.

Supplementary Table 1. Associations of tumor infiltrating lymphocyte scores and survival outcomes in Black women with breast cancer from the Women's Circle of Health Study

	# events/total number of patients	HR (95% CI)	P-value
a. All-cause mortality			
Per 10% increase in TIL score	104/688	0.86 (0.78-0.95)	0.003
TIL score in categories			
<10%	31/197	1.00	
10-50%	60/382	0.71 (0.45-1.12)	0.14
50-100%	13/109	0.38 (0.19-0.76)	0.006
b. Disease-specific mortality			
Per 10% increase in TIL score	71/688	0.90 (0.80-1.01)	0.06
TIL score in categories			
<10%	18/197	1.00	
10-50%	44/382	0.84 (0.48-1.49)	0.54
50-100%	9/109	0.50 (0.21-1.08)	0.08

Footnote: Associations of pathological tumor infiltrating immune lymphocyte (TIL) scores with all-cause mortality and disease-specific mortality in Black breast cancer patients in the Women's Circle of Health Study (WCHS). Hazards ratios (HRs) and 95% confidence intervals (CIs) for all-cause mortality were derived from Cox proportional hazards models with adjustment for age at diagnosis, cancer stage, grade, and hormone receptor status. Sub-distribution HRs (SHRs) and 95% CIs for disease-specific mortality were derived from competing risk models where death from non-breast cancer causes were treated as competing risk with adjustment for the same set of covariates.

Supplementary Table 2. Associations of ExCD8-r signature with all-cause mortality in breast cancer patients

ExCD8-r	Overall cohort			HR-positive			HR-negative		
	# events/total	HR (95% CI)	P	# events/total	HR (95% CI)	P	# events/total	HR (95% CI)	P
WCHS									
Low	21/151	1.00		7/66	1.00		18/83	1.00	
High	40/169	1.87 (1.09 - 3.22)	0.02	14/80	1.95 (0.77 - 4.91)	0.16	22/91	1.13 (0.60 - 2.13)	0.71
TCGA									
Low	47/353	1.00		26/267	1.00		18/71	1.00	
Intermediate	47/354	1.10 (0.71 - 1.71)	0.66	34/266	1.49 (0.87 - 2.55)	0.14	12/71	0.77 (0.37 - 1.61)	0.25
High	53/351	1.55 (1.01 - 2.39)	0.05	39/264	2.33 (1.37 - 3.96)	0.002	8/70	0.72 (0.28 - 1.82)	0.51
METABRIC									
Low	306/635	1.00		234/493	1.00		68/142	1.00	
Intermediate	360/635	1.14 (0.98 - 1.33)	0.09	280/493	1.18 (0.99 - 1.41)	0.06	85/142	1.14 (0.82 - 1.58)	0.43
High	437/634	1.26 (1.08 - 1.46)	0.002	351/492	1.27 (1.07 - 1.51)	0.005	85/142	0.98 (0.70 - 1.37)	0.91

Footnote: ExCD8-r signature levels are categorized into binary in Women's Circle of Health Study (WCHS) based on the median due to limited sample size. The signature levels are categorized into tertiles in The Cancer Genome Atlas (TCGA) and Molecular Taxonomy of Breast Cancer International Consortium (METABRIC) datasets. Hazards ratios (HRs) and 95% confidence intervals (CIs) are derived from Cox proportional hazards models with adjustment for age at diagnosis and clinical prognostic factors available from each dataset, namely cancer stage, grade, and hormone receptor (HR) status in WCHS; cancer stage and hormone receptor status in TCGA; tumor size, Nottingham prognostic index, and HR status in METABRIC.

Supplementary Table 3. Associations of ExCD8-r signature with disease-specific mortality in breast cancer patients

ExCD8-r	Overall cohort			HR-positive			HR-negative		
	# events/total	HR (95% CI)	P	# events/total	HR (95% CI)	P	# events/total	HR (95% CI)	P
WCHS									
Low	12/152	1.00		3/67	1.00		11/83	1.00	
High	22/170	1.76 (0.88 - 3.55)	0.11	7/81	2.06 (0.56 - 7.62)	0.28	13/91	1.13 (0.49 - 2.65)	0.77
TCGA									
Low	28/345	1.00		15/264	1.00		11/66	1.00	
Intermediate	24/347	1.03 (0.57 - 1.88)	0.91	14/260	1.13 (0.53 - 2.43)	0.75	9/71	0.95 (0.36 - 2.48)	0.92
High	30/348	1.50 (0.83 - 2.73)	0.18	21/261	2.21 (1.10 - 4.44)	0.03	6/70	1.19 (0.41 - 3.40)	0.75
METABRIC									
Low	172/635	1.00		119/493	1.00		53/142	1.00	
Intermediate	223/635	1.27 (1.03 - 1.57)	0.02	155/493	1.29 (1.02 - 1.65)	0.04	72/142	1.44 (0.99 - 2.09)	0.06
High	227/634	1.28 (1.05 - 1.57)	0.02	171/492	1.44 (1.14 - 1.82)	0.003	52/142	0.90 (0.61 - 1.32)	0.58

Footnote: ExCD8-r signature levels are categorized into binary in Women's Circle of Health Study (WCHS) based on the median due to limited sample size. The signature levels are categorized into tertiles in The Cancer Genome Atlas (TCGA) and Molecular Taxonomy of Breast Cancer International Consortium (METABRIC) datasets. Hazards ratios (HRs) and 95% confidence intervals (CIs) are derived from Cox proportional hazards models with adjustment for age at diagnosis and clinical prognostic factors available from each dataset, namely cancer stage, grade, and hormone receptor (HR) status in WCHS; cancer stage and hormone receptor status in TCGA; tumor size, Nottingham prognostic index, and HR status in METABRIC. Sub-distribution HRs (SHRs) and 95% CIs for disease-specific mortality were derived from competing risk models where death from non-breast cancer causes were treated as competing risk with adjustment for the same set of covariates.

Supplementary Table 4. Associations of $CD8^+$ T cell absolute fractions and the combined CD8-ExCD8-r signature with all-cause mortality and disease-specific mortality in hormonal receptor (HR) negative breast cancer patients in METABRIC

	All-cause mortality			Disease-specific mortality		
	# events/total	HR (95% CI)	P	# events/total	HR (95% CI)	P
$CD8^+$ T cell absolute fractions						
Low	134/213	1.00		104/213	1.00	
High	104/213	0.65 (0.50 - 0.85)	0.001	73/213	0.62 (0.46 - 0.85)	0.003
Combined CD8-ExCD8-r signature						
$CD8^{high}ExCD8\text{-}r^{low}$	57/119	1.00		44/119	1.00	
$CD8^{high}ExCD8\text{-}r^{high}$	47/94	0.77 (0.51 - 1.14)	0.19	29/94	0.80 (0.50 - 1.28)	0.36
$CD8^{low}ExCD8\text{-}r^{low}$	53/94	1.19 (0.81 - 1.75)	0.36	44/94	1.36 (0.89 - 2.09)	0.16
$CD8^{low}ExCD8\text{-}r^{high}$	81/119	1.49 (1.05 - 2.10)	0.02	60/119	1.54 (1.02 - 2.31)	0.04

Footnote: Both the $CD8^+$ T cell absolute fractions and ExCD8-r signature levels are categorized into binary based on the median. Hazards ratios (HRs) and 95% confidence intervals (CIs) are derived from Cox proportional hazards models with adjustment for age at diagnosis and clinical prognostic factors including tumor size, Nottingham prognostic index, and HR status in Molecular Taxonomy of Breast Cancer International Consortium (METABRIC). Sub-distribution HRs (SHRs) and 95% CIs for disease-specific mortality were derived from competing risk models where death from non-breast cancer causes were treated as competing risk with adjustment for the same set of covariates.

Supplementary Figure 1. Correlation plot of pathological and molecular scores of infiltrating immune cells in breast cancer patients from the Women's Circle of Health Study

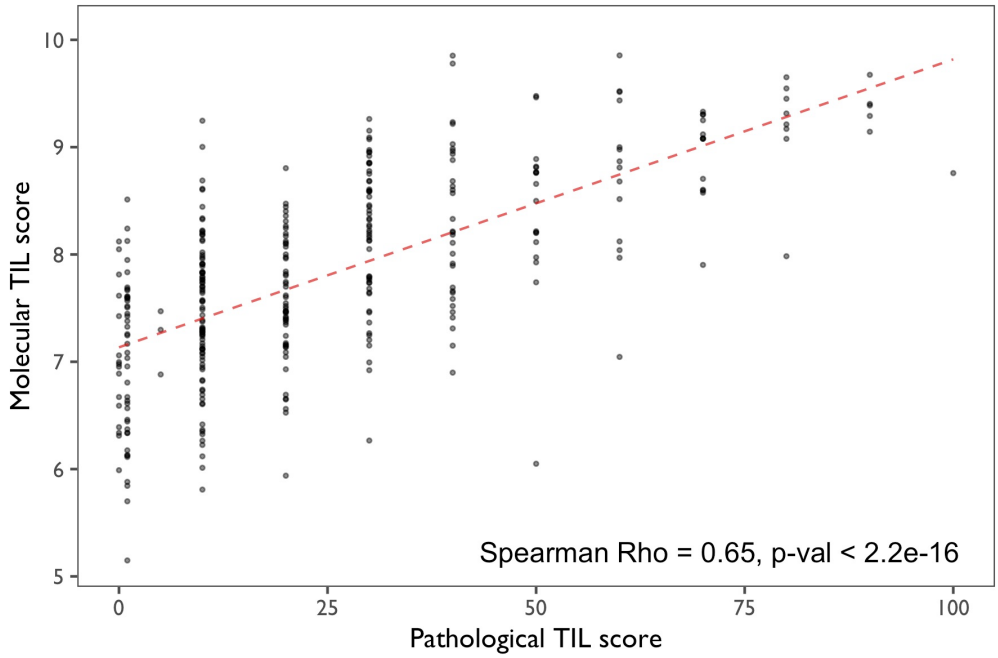

Figure legend: Pathological TILs were scored between 0% and 100% in increments of 10%. Molecular TIL scores were estimated based on tumor gene expression data from the same patients. Each dot represents one patient and the red dashed line is the linear regression line, with Spearman correlation coefficient and p-value shown at the bottom.

Supplementary Figure 2. CONSORT flow diagram of the study design, cohorts and major analyses performed

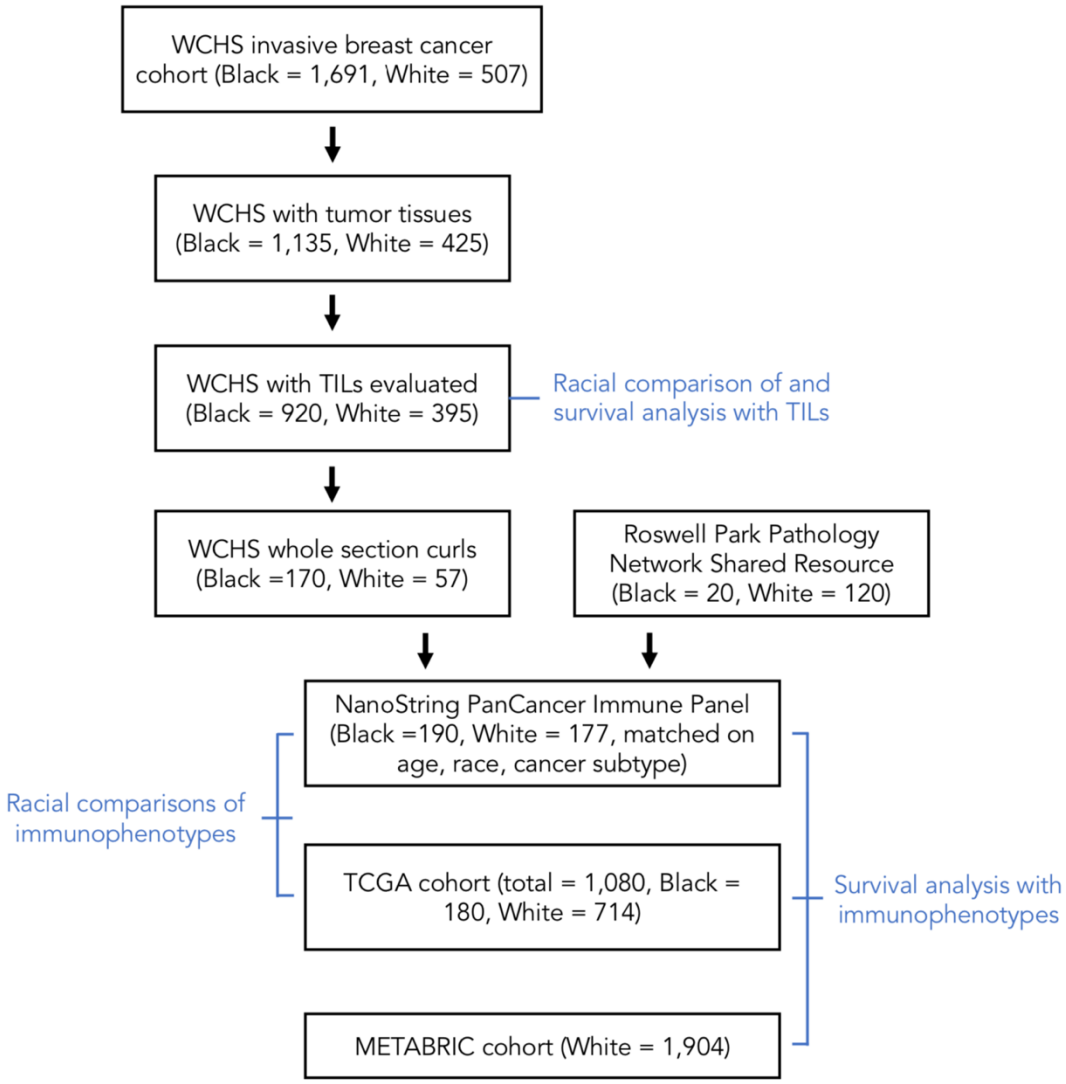

Abbreviations: TCGA: The Cancer Genome Atlas; METABRIC: Molecular Taxonomy of Breast Cancer International Consortium; TILs: tumor infiltrating lymphocytes; WCHS: Women's Circle of Health Study

Supplementary Figure 3. Pathological tumor infiltrating lymphocyte scores by tumor hormone receptor and HER2 status in breast cancer patients from the Women's Circle of Health Study

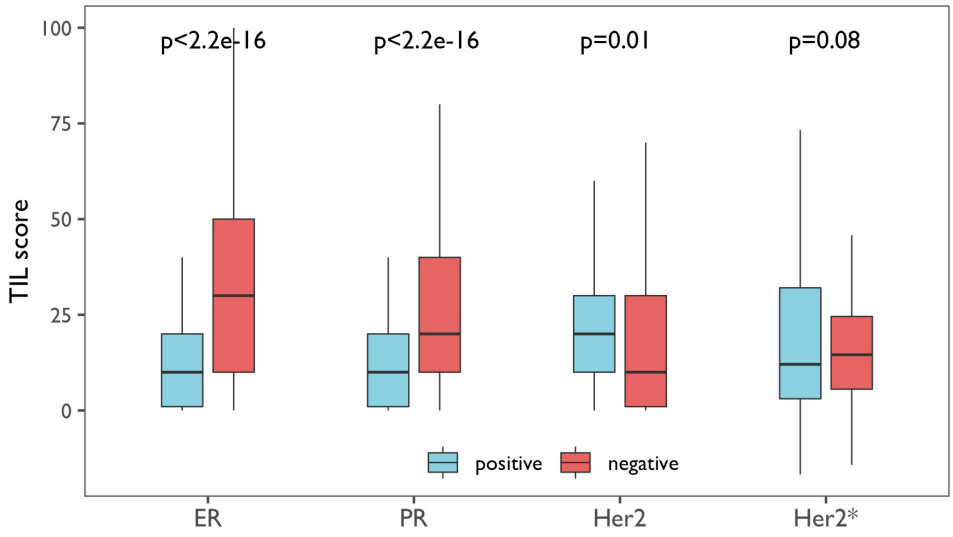

Figure legend: The boxplot shows pathological tumor infiltrating lymphocyte (TIL) scores by tumor estrogen receptor (ER), progesterone receptor (PR), and human epithelial growth factor receptor 2 (HER2) status. The bar in the middle of a box indicates the subgroup median, and the lower and upper edges indicate the first and third quartiles, respectively. The extended lines indicate the range in each subgroup. P-values were derived from Wilcoxon test between Black and White patients. Her2* indicates the results with adjustment for tumor ER/PR status, which was not statistically significant

Supplementary Figure 4. Associations of the absolute and relative fractions of immune cells with breast tumor hormone receptor and HER2 status

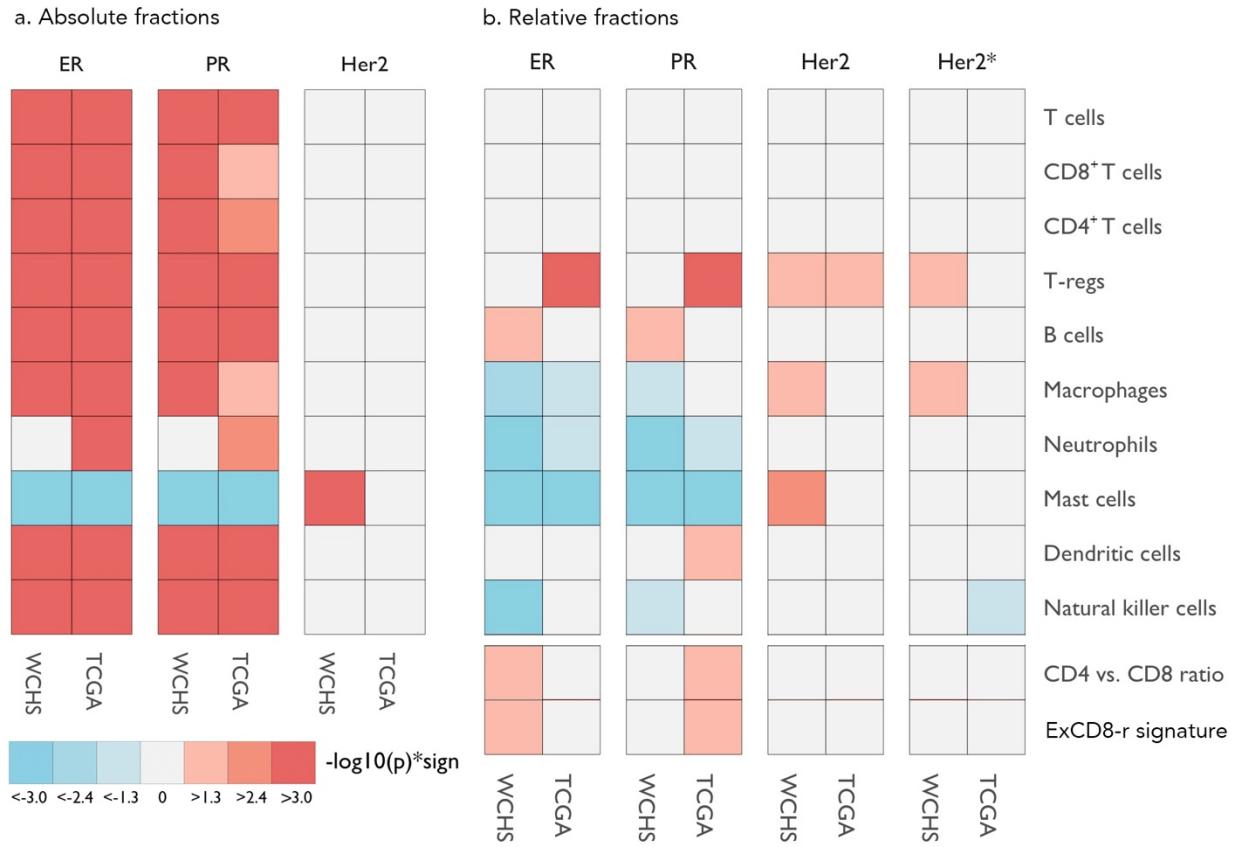

Figure legend: The table plots show the log10-transformed p-values of the differences in the absolute fractions (panel a) and relative fractions (panel b) of 10 major immune cell subsets by tumor estrogen receptor (ER), progesterone receptor (PR), and human epithelial growth factor receptor 2 (HER2) status. Red colors indicate the sign of differences to be higher in the receptor positive tumors and blue colors indicate the sign of the differences to be higher in the receptor negative tumors. Results from Women's Circle of Health Study (WCHS) and The Cancer Genome Atlas (TCGA) are plotted side-by-side for cross-validation. Log10(p) of 1.3, 2.4 and 3.0 correspond to the p-value cutoffs without adjustment for multiple testing and with adjustment for 10 tests (10 major immune cell subsets) and 50 tests (10 immune cell subsets plus 2 ratios times 2 different fractions [absolute and relative] times 2 tumor markers (ER/PR and HER2). Her2* indicates the results with adjustment for tumor ER/PR status.

Supplementary Figure 5. The relative fractions of immune cell subsets in Black and White breast cancer patients

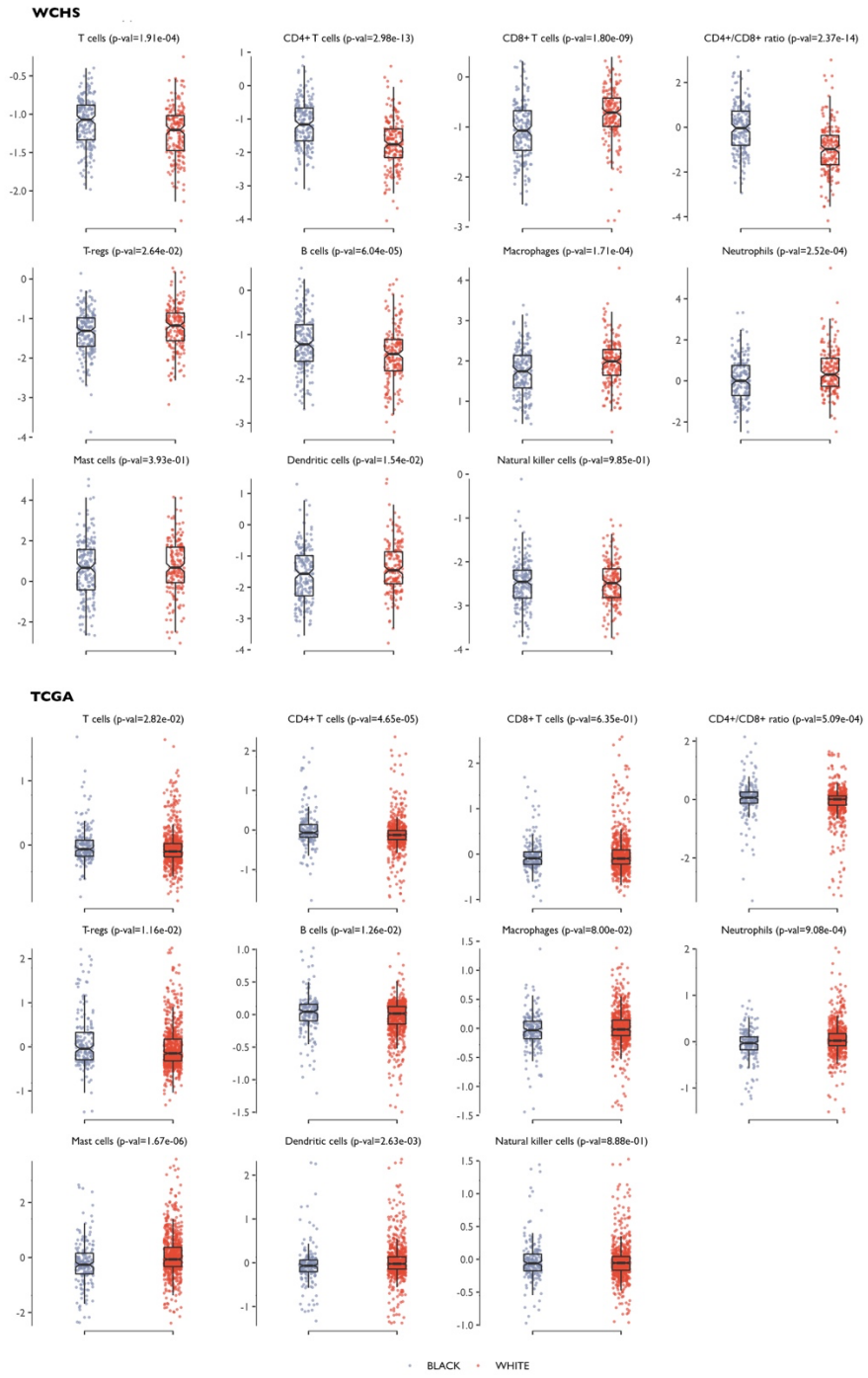

Footnote: Boxplots of the relative fractions of immune cell subsets in Black and White breast cancer patients. The bar in the middle of a box indicates the subgroup median, and the lower and upper edges indicate the first and third quartiles, respectively. The extended lines indicate the range in each subgroup. Results from Women's Circle of Health Study (WCHS) are shown in the top panel, and results from the Cancer Genome Atlas (TCGA) are shown in the bottom panel and results from.

Supplementary Figure 6. The relative fractions of immune cell subsets in Black and White breast cancer patients after adjustment for tumor hormone receptor status

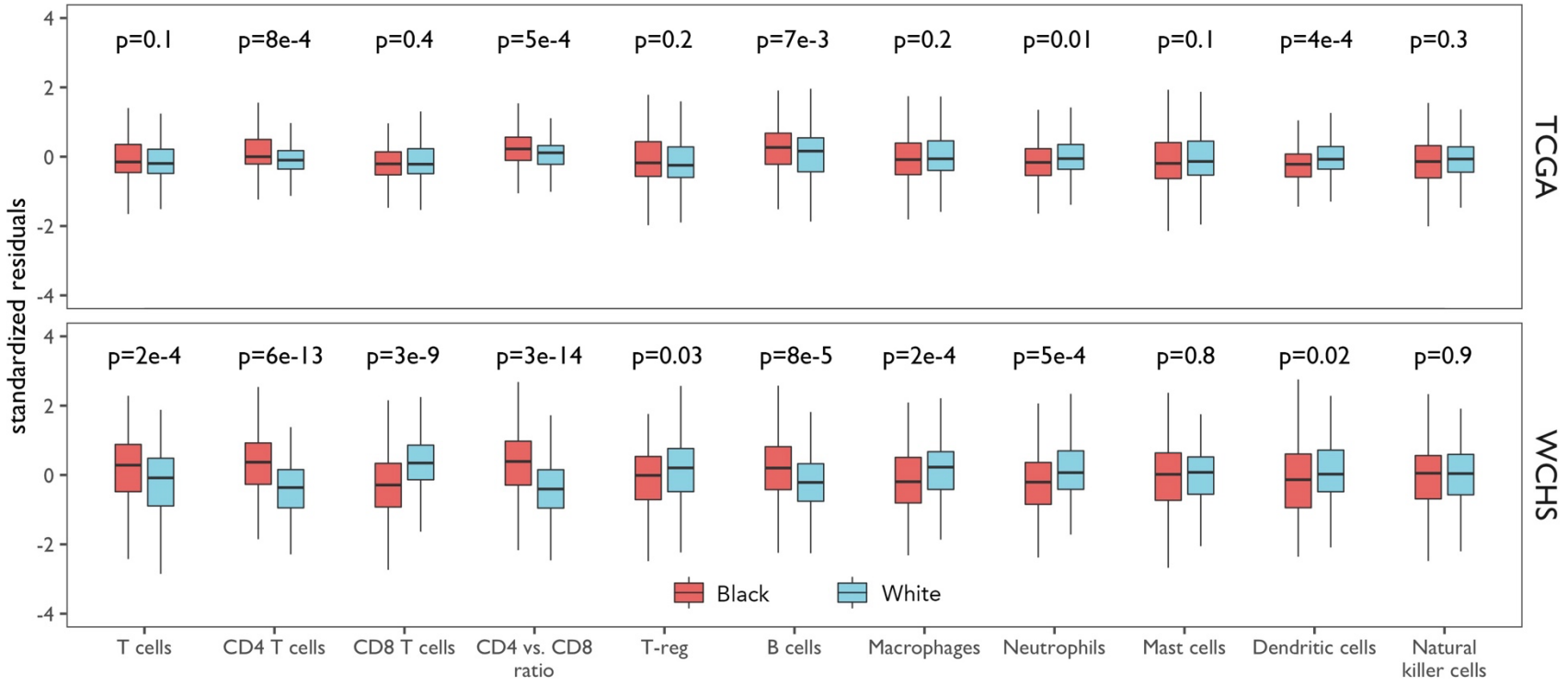

Figure legend: Boxplots of standardized residuals of the relative fractions of immune cell subsets after adjusting for tumor hormone receptor (HR) status in Black and White breast cancer patients. The bar in the middle of a box indicates the subgroup median, and the lower and upper edges indicate the first and third quartiles, respectively. The extended lines indicate the range in each subgroup. Results from The Cancer Genome Atlas (TCGA) are shown in the top panel and results from Women's Circle of Health Study (WCHS) are shown in the bottom panel. Standardized residuals and p-values of race (Black vs. White) were derived from multivariable linear regression models with adjustment for tumor HR status.

Supplementary Figure 7. Racial differences in the relative fractions of immune cell subsets in Black and White breast cancer patients stratified by tumor hormone receptor status

A. HR-positive tumor subtype

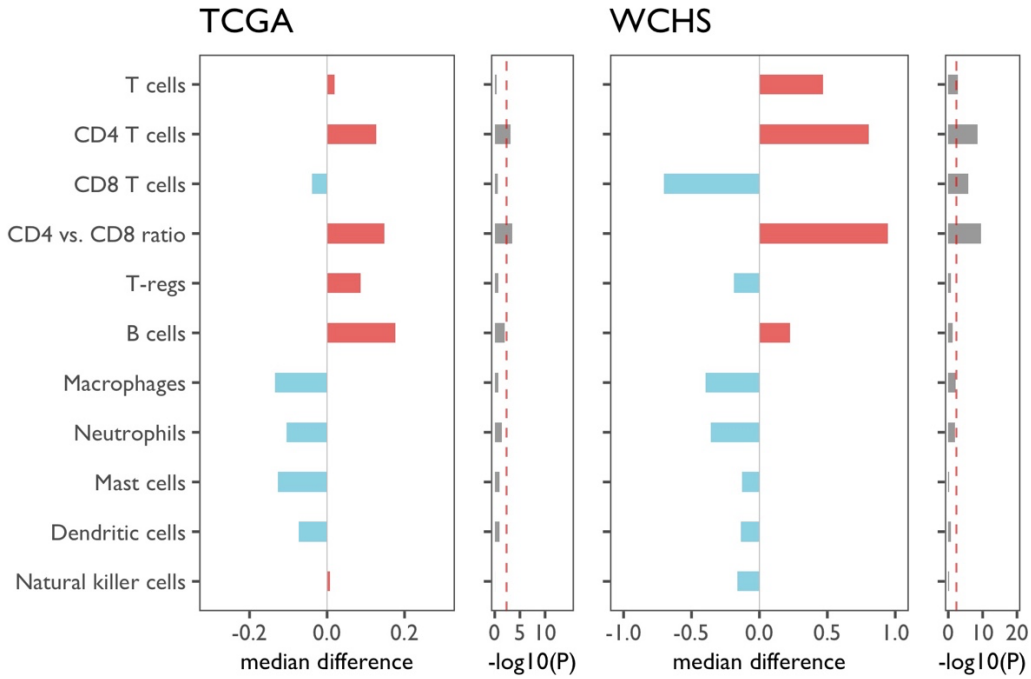

B. HR-negative tumor subtype

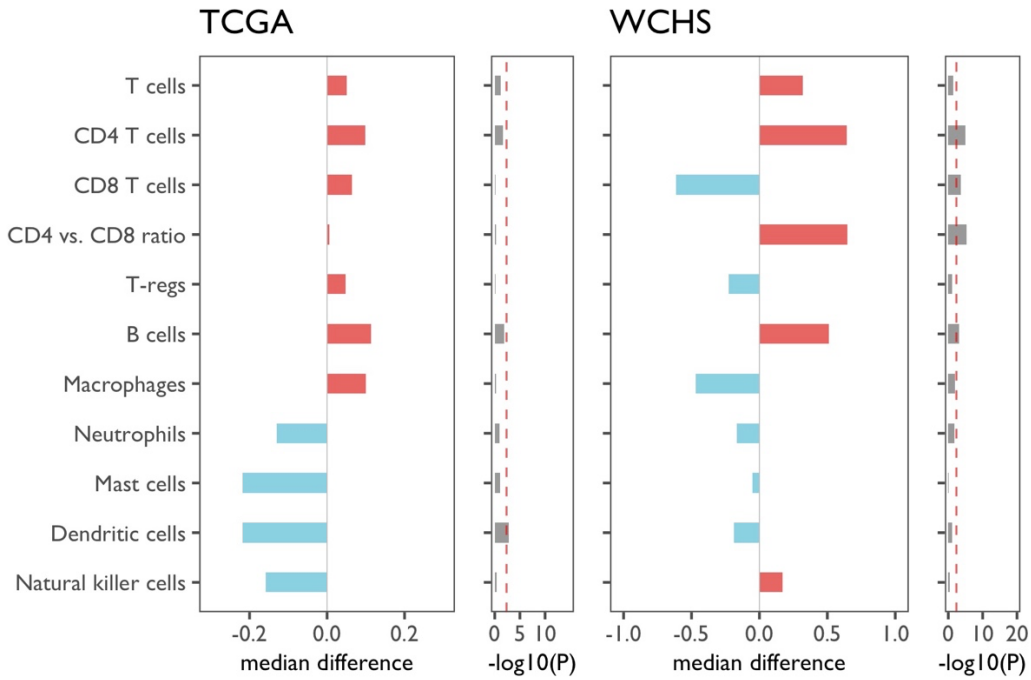

Figure legend: Relative fractions of the 10 major immune cell subsets plus $CD4^+$ to $CD8^+$ T cell ratios were centered to an overall mean of 0 before subgroup medians were calculated for Whites and Blacks. The differences in subgroup medians are plotted in bar graphs, with red color

indicating higher immune cell estimates in Blacks and blue color indicating higher estimates in Whites. P-values from Wilcoxon test were log10-transformed, negated and plotted as bar graphs along the median differences. The red reference line indicates a cutoff of significance level after adjusting for multiple testing [-log10(0.05/11) = 2.3]. Patient populations from Women's Circle of Health Study (WCHS) and The Cancer Genome Atlas (TCGA) were included for cross validation.

Supplementary Figure 8. Analysis of CD4+ T cells using immunohistochemical staining

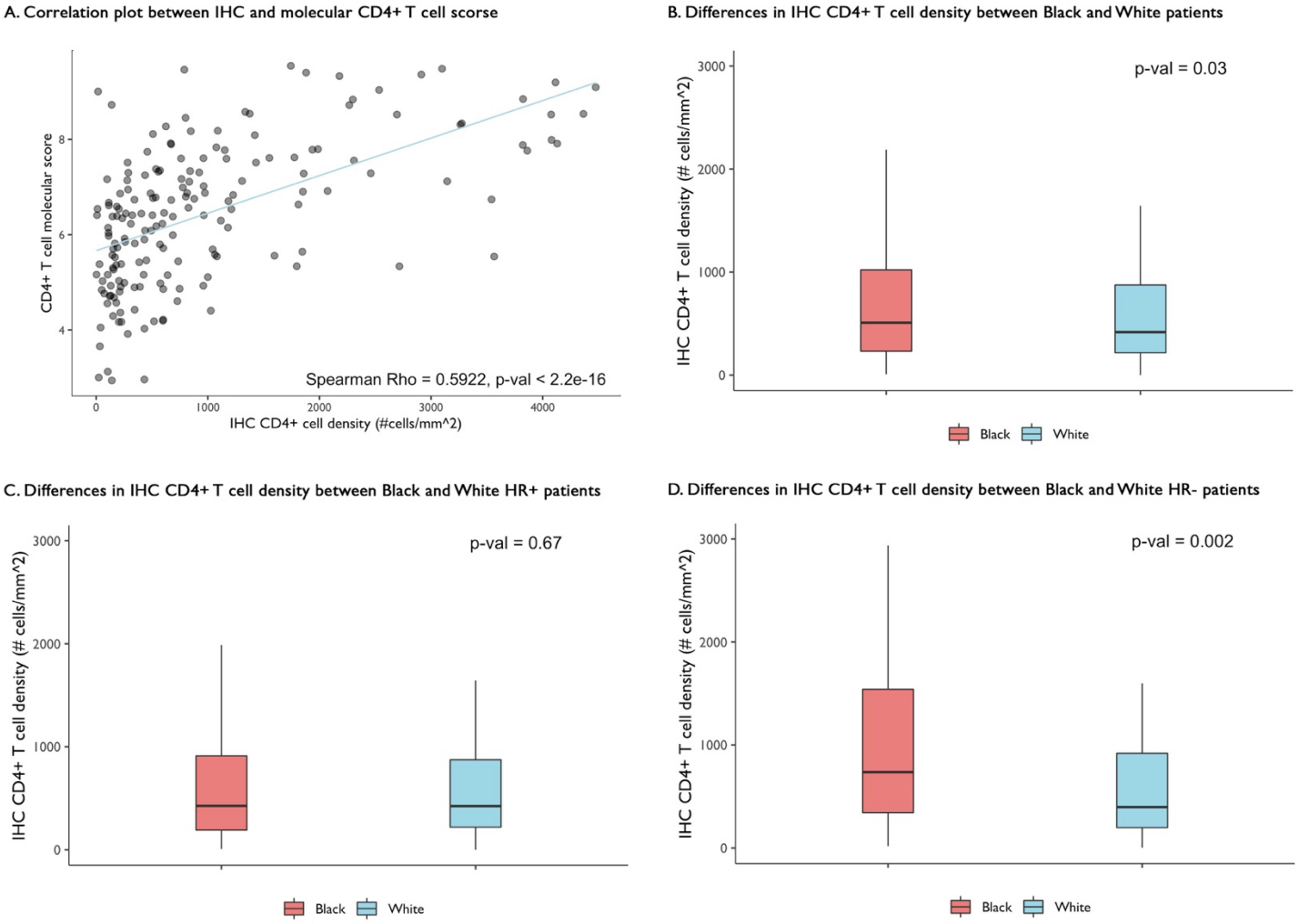

Figure legend: A). Correlation plot between molecular score and immunohistochemical (IHC) staining of CD4 in breast tumor tissues. Each dot represents one patient and the red dashed line is the linear regression line, with Spearman correlation coefficient and p-value shown at the bottom. **B).** Racial differences in CD4+ T cell density between Black and White patients. **C).** Racial differences in CD4+ T cell density between Black and White patients with hormonal receptor (HR) positive cancer. **D).** Racial differences in CD4+ T cell density between Black and White patients with HR negative cancer.

Supplementary Figure 9. Racial differences in the relative fractions of $CD4^+$ follicular helper cells between Black and White breast cancer patients after adjustment for tumor hormone receptor status

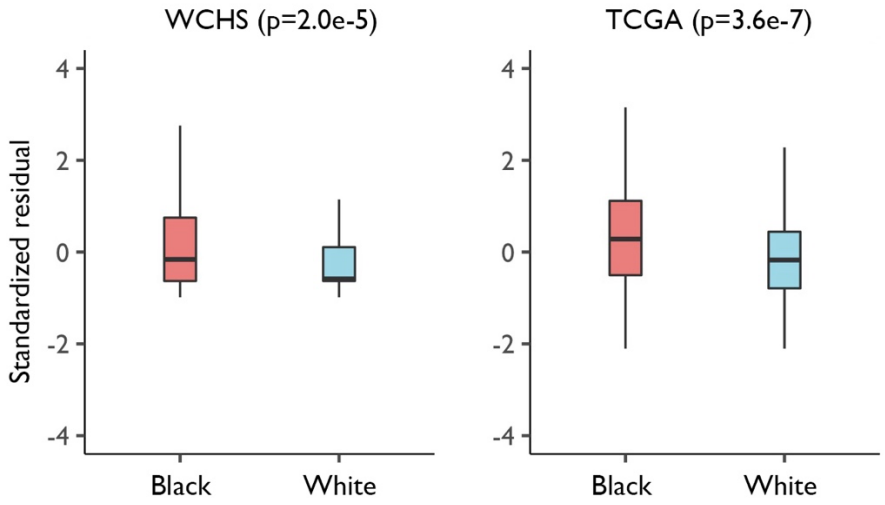

Figure legend: Boxplots of standardized residuals of the relative fractions of $CD4^+$ follicular helper cells after adjusting for tumor hormone receptor (HR) status in Black and White breast cancer patients. The bar in the middle of a box indicates the subgroup median, and the lower and upper edges indicate the first and third quartiles, respectively. The extended lines indicate the range in each subgroup. Results from The Cancer Genome Atlas (TCGA) are shown on the left and results from Women's Circle of Health Study (WCHS) are shown on the right. Standardized residuals and p-values of race (Black vs. White) were derived from multivariable linear regression models with adjustment for tumor HR status.

Supplementary Figure 10. Racial differences in immune receptor repertoire between Black and White breast cancer patients in The Cancer Genome Atlas

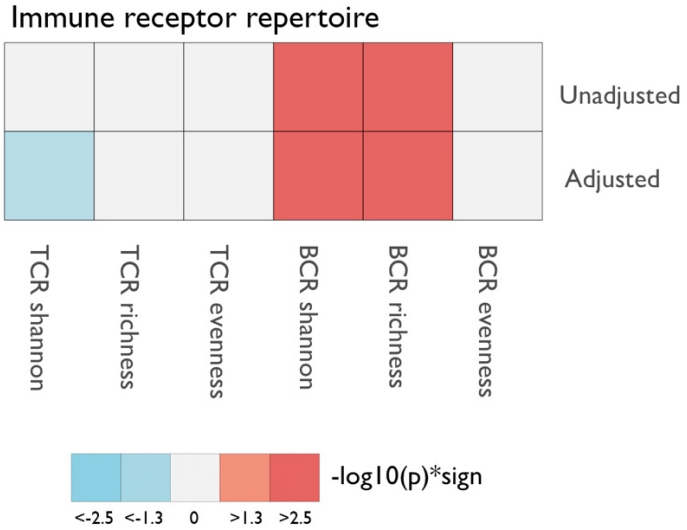

Figure legend: The table plots show the log10-transformed p-values of the differences between Black and White breast cancer patients in the estimates of immune receptor repertoire for T cell receptor (TCR) and B cell receptor (BCR), from the unadjusted linear models and the models with adjustment for tumor hormone receptor status. Red colors indicate the sign of differences to be higher in the receptor positive tumors and blue colors indicate the sign of the differences to be higher in the receptor negative tumors. Log10(p) of 1.3 and 2.5 correspond to the p-value cutoffs without adjustment for multiple testing and with adjustment for 12 tests (6 indices times two models).

Supplementary Figure 11. Correlations of $CD4^+$ T cell fractions, B cell fractions and B-cell receptor repertoire in The Cancer Genome Atlas

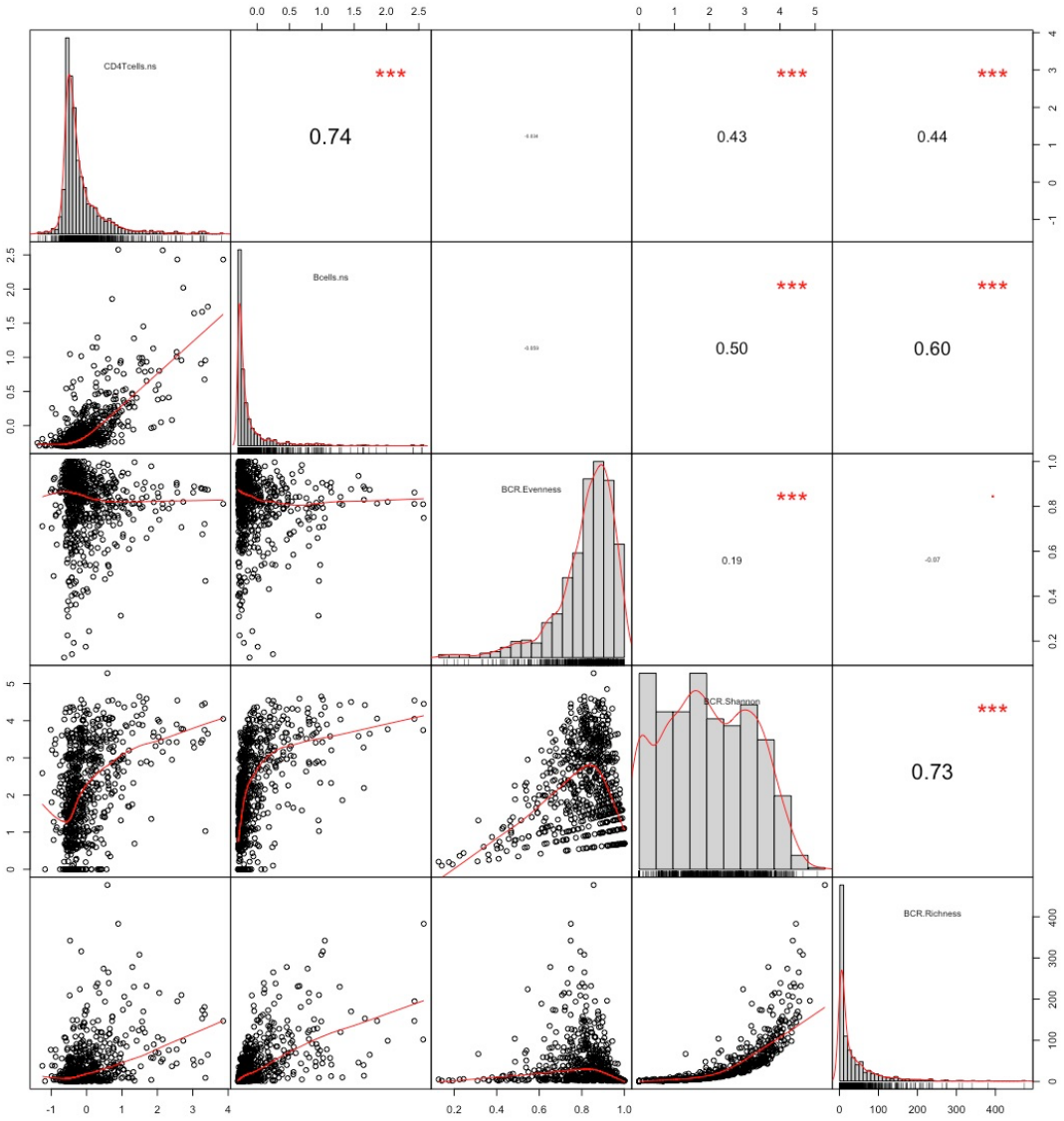

Figure legend: The correlation plot shows histograms of $CD4^+$ T cell fractions and indices of immune receptor repertoire on the diagonal, scatter plots with regression lines on the lower quadrant, and Spearman correlation coefficients on the upper quadrant. *** indicates the p-value <0.001.

Supplementary Figure 12. Co-expression patterns of inhibitory receptors in breast tumors

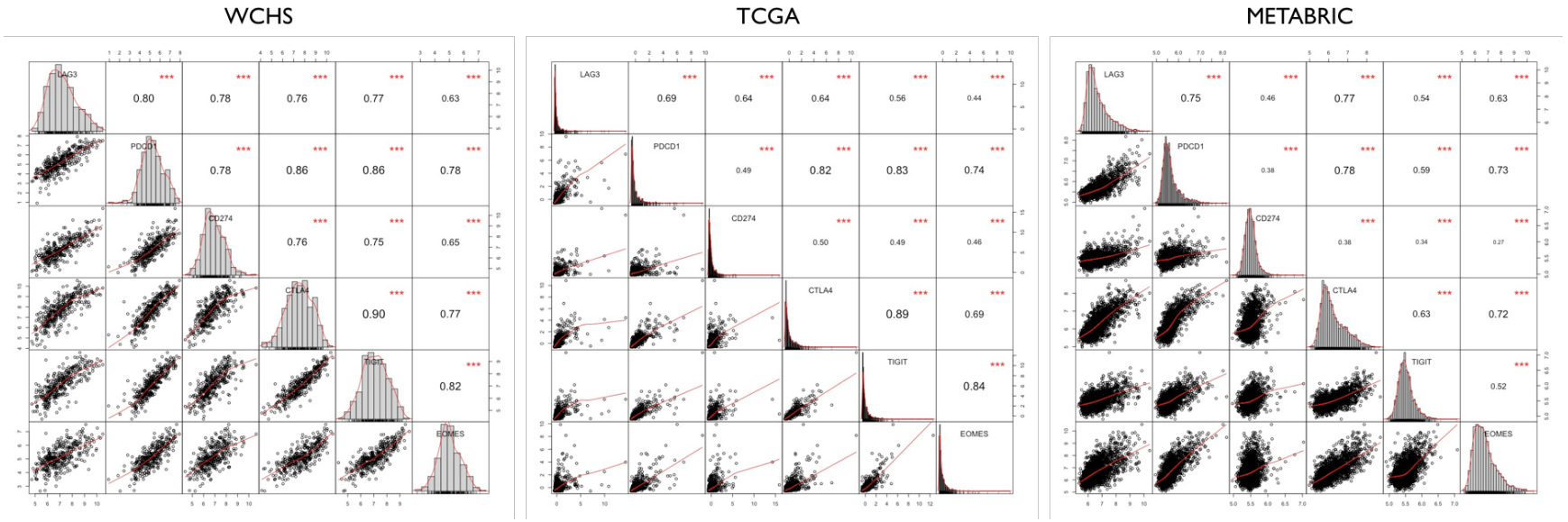

Figure legend: The correlation plot shows histograms of gene expression levels on the diagonal, scatter plots with regression lines on the lower quadrant, and Spearman correlation coefficients on the upper quadrant. *** indicates the p-value <0.001. WCHS, Women's Circle of Health Study; TCGA, The Cancer Genome Atlas; METABRIC, Molecular Taxonomy of Breast Cancer International Consortium.

Supplementary Figure 13. Racial differences in the expression of inhibitory receptors and ExCD8-r signature between Black and White breast cancer patients after adjustment for tumor hormone receptor status

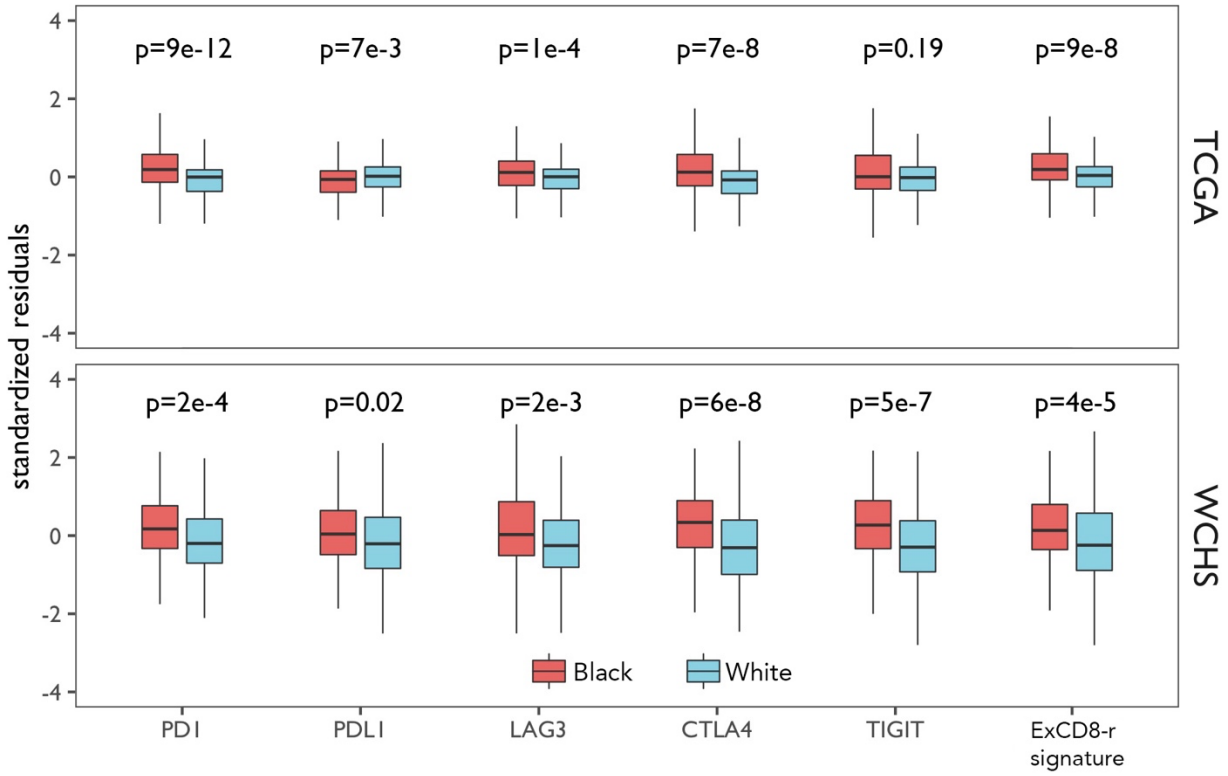

Figure legend: Boxplots of standardized residuals of the expression of inhibitory receptors relative to the absolute fractions of $CD8^+$ T cells and the ExCD8-r signature after adjusting for tumor hormone receptor (HR) status in Black and White breast cancer patients. The bar in the middle of a box indicates the subgroup median, and the lower and upper edges indicate the first and third quartiles, respectively. The extended lines indicate the range in each subgroup. Results from The Cancer Genome Atlas (TCGA) are shown in the top panel and results from Women's Circle of Health Study (WCHS) are shown in the bottom panel. Standardized residuals and p-values of race (Black vs. White) were derived from multivariable linear regression models with adjustment for tumor HR status.

Supplementary Figure 14. Analysis of a previously developed T cell exhaustion signature by Cai et al. (*J Pathol 2020*)

A. Correlation between the previous T cell exhaustion signature and the signature developed in this study (without adjusting for CD8+ T cell scores) in the WCHS dataset

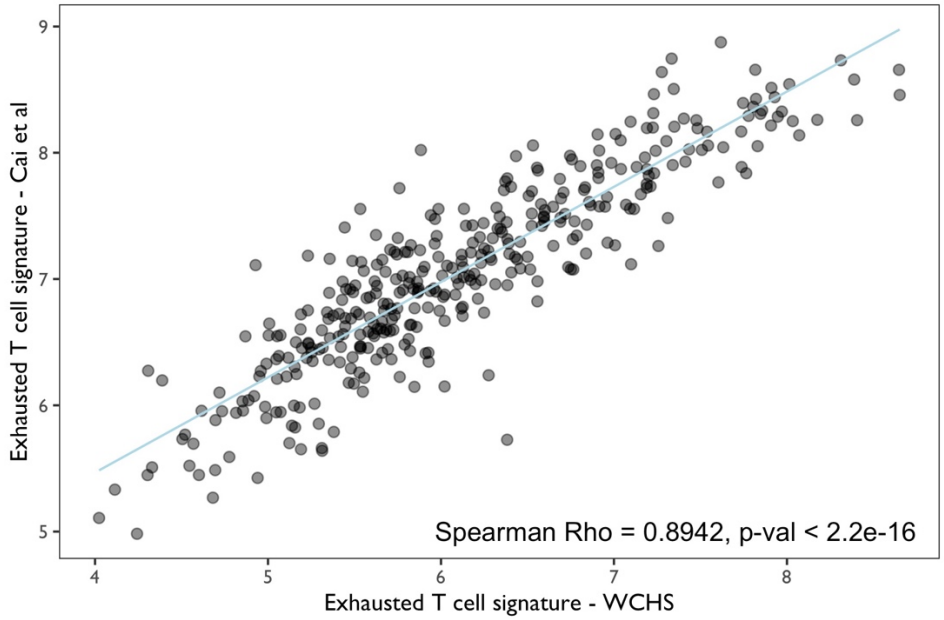

B. Racial differences in T cell exhaustion signature scores by Cai et al between Black and White breast cancer patients

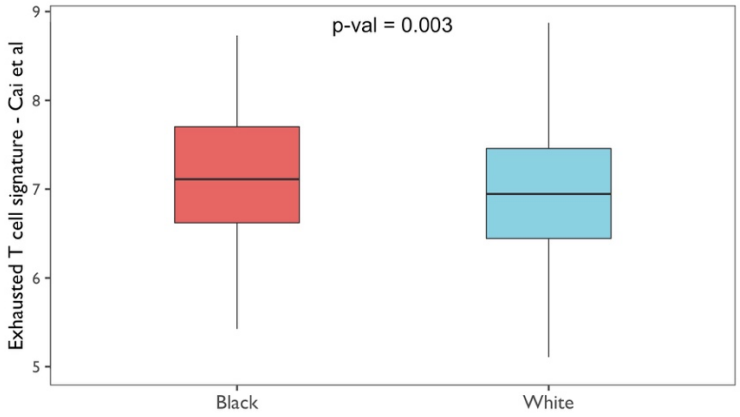

Figure legend: A). Each dot represents one patient and the red dashed line is the linear regression line, with Spearman correlation coefficient and p-value shown at the bottom. **B).** Racial differences in T cell exhaustion signature score defined by Cai et al between Black and White breast cancer patients.

Supplementary Figure 14. Kaplan-Meir survival curves of disease-specific mortality by ExCD8-r signature

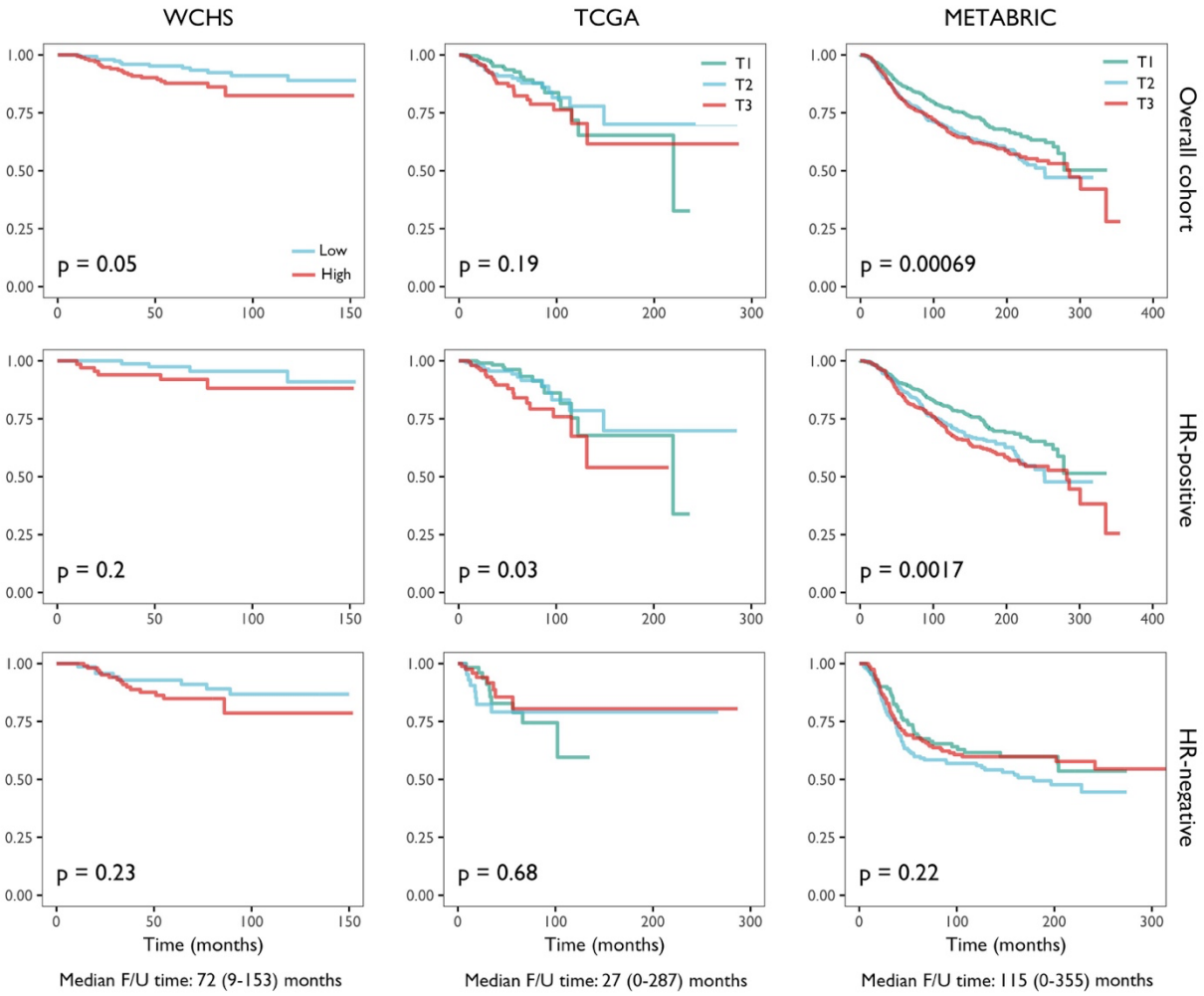

Figure legend: Kaplan-Meier survival curves of breast cancer-specific mortality by the levels of ExCD8-r signature are plotted for Women's Circle of Health Study (WCHS), The Cancer Genome Atlas (TCGA) and Molecular Taxonomy of Breast Cancer International Consortium (METABRIC) datasets, with and without stratification by tumor hormone receptor (HR) status. The signature levels in WCHS were categorized into binary based on the median due to limited sample size and categorized into thirds in TCGA and METABRIC datasets with large sample sizes. P-values from log-rank test are displayed within the plots. The medians and ranges of the follow-up (F/U) time are shown at the bottom. The analyses were conducted with all races combined due to limited sample size of Black patients in the cohorts.

Supplementary Figure 15. Kaplan-Meir survival curves of all-cause mortality and disease-specific mortality by $CD8^+$ T cell estimates and the ExCD8-r signature in hormonal receptor (HR) negative breast cancer patients in METABRIC

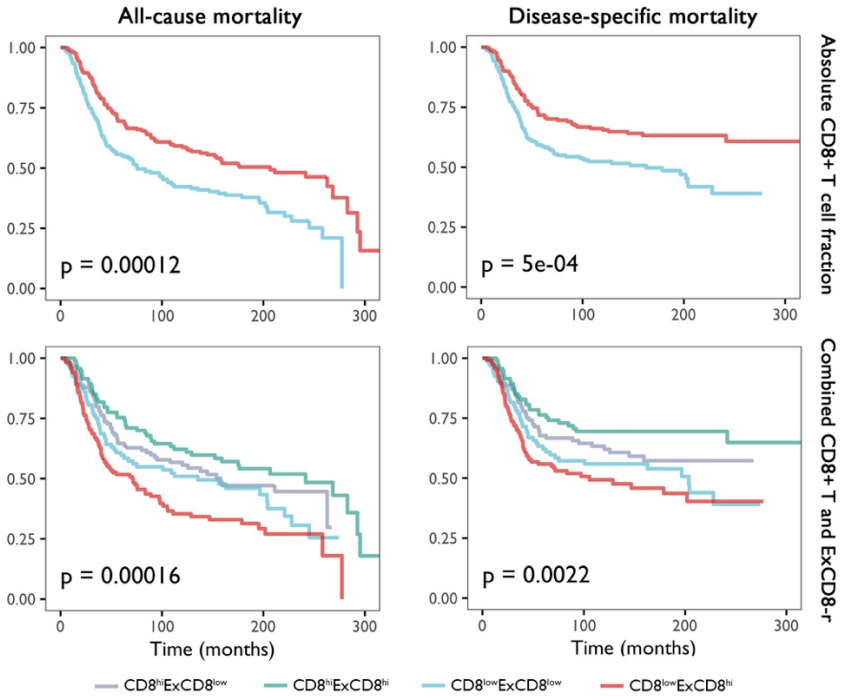

Figure legend: Kaplan-Meier survival curves of all-cause mortality and disease-specific mortality by the absolute fractions of $CD8^+$ T cells (top panels) and the combination of the absolute fractions of $CD8^+$ T cells and the ExCD8-r signature (bottom panel) are plotted for the hormone receptor (HR)-negative subcohort from Molecular Taxonomy of Breast Cancer International Consortium (METABRIC. P-values from log-rank test are displayed within the plots.

Supplementary Figure 16. Subgroups defined by $CD8^+$ T cell estimates and ExCD8-r signature in Black and White breast cancer patients stratified by tumor hormone receptor status

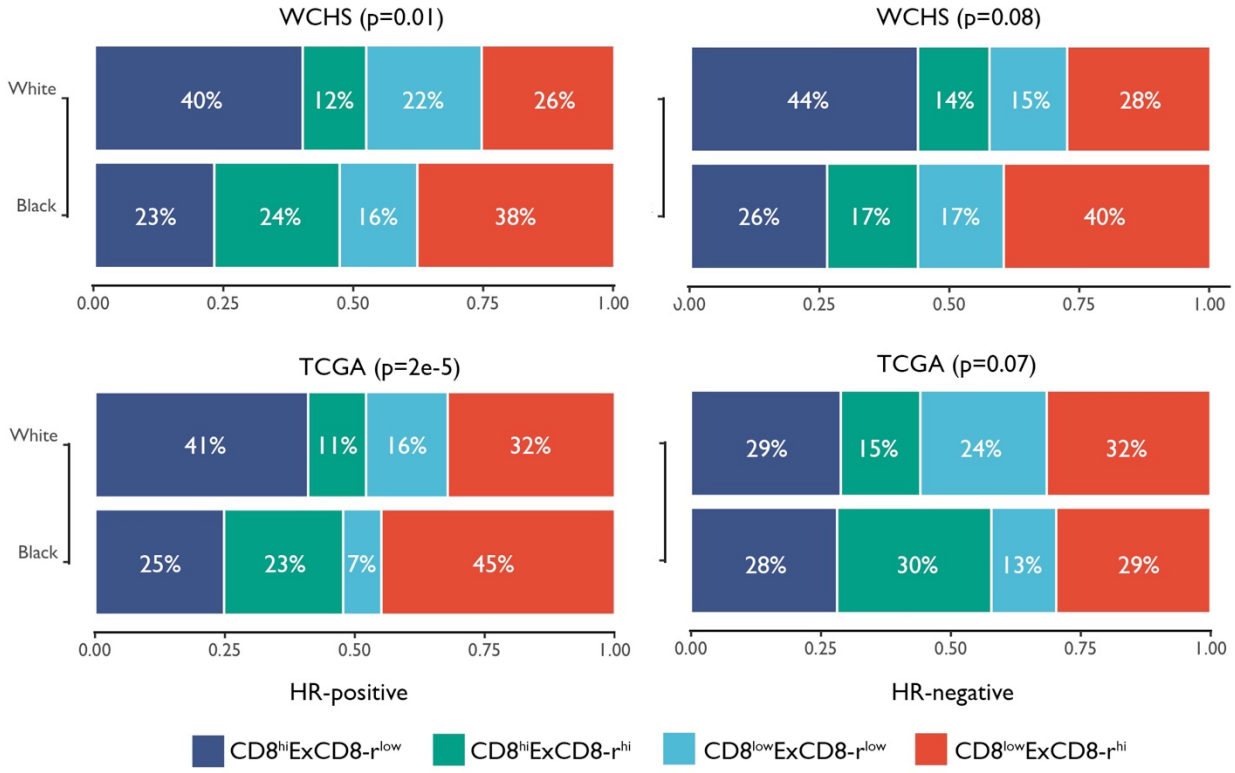

Figure legend: Stacked bar graphs of the proportions of the four patient subgroups defined on the basis of the combination of the absolute fractions of $CD8^+$ T cells and the ExCD8-r signature in Black and White breast cancer patients, stratified by hormone receptor (HR)-positive and HR-negative cancer subtype. The bar height of each subgroup corresponds to the percentage of that group within the racial group. P-values from Chi-square test between subgroup and race are displayed for Women's Circle of Health Study (WCHS) and The Cancer Genome Atlas (TCGA) data sets.